Stanier, S. A. *et al.* (2014). *Géotechnique* **64**, No. 11, 918–926 [http://dx.doi.org/10.1680/geot.14.P.003]

**TECHNICAL NOTE**

# Observing the effects of sustained loading on spudcan footings in clay

S. A. STANIER*, R. RAGNI*, B. BIENEN* and M. J. CASSIDY*

Spudcan foundations of mobile jack-up rigs are penetrated into the seabed under seawater ballast preload, which is shed prior to rig operations commencing. During pauses in the installation process and during operation, soil beneath the spudcan foundations stiffens and strengthens due to consolidation. On the application of further loading or during spudcan extraction, this causes increased resistance, which in extremis can result in punch-though type failure. This note reports results from a series of experiments with particle image velocimetry measurements that were performed in a drum centrifuge to facilitate observation of the effects of a load-hold period on the soil movements around a model spudcan during subsequent further loading. The results show that the dimensionless load-hold period dominates the enhancement in the penetration resistance, due to significantly more soil being mobilised following a long load-hold period. These observations might be useful to (*a*) predict the enhancement in bearing capacity factor due to a load-hold period during installation or operation and (*b*) predict the footing extraction resistance during jack-up re-deployment.

KEYWORDS: bearing capacity; consolidation; offshore engineering; soil/structure interaction; time dependence

## INTRODUCTION

Spudcan foundations of mobile jack-up rigs are penetrated into the seabed under seawater ballast preload, which is shed prior to rig operations commencing. This process is often discontinuous, with breaks in preloading caused by inclement weather and other technical problems. Fig. 1 illustrates schematically a time history of the process of jack-up installation. Soil beneath the footing is subjected to significant loads during these pauses, causing consolidation of the soil around the footing, resulting in strengthening and stiffening. In practice offshore, hold periods as short as a few hours have been reported to have resulted in 'punch-through' type failure (defined as 'rapid, uncontrolled vertical leg movement due to soil failure in strong overlying weak soil' in ISO (2012)) upon subsequent further loading, even in soil where punch-through was not an anticipated risk, such as in normally consolidated clay (Brennan *et al.*, 2006).

For this scenario, Bienen & Cassidy (2013) provided design charts – back-calculated from centrifuge experiments – to allow estimation of the enhancement of the effective bearing capacity factor, $N_c^*$, for a range of dimensionless load-hold periods. The charts cover the range anticipated for short-term pauses in jack-up installation and longer-term operational periods of up to a few years. Such charts are useful to predict the increase in penetration resistance due to pauses in the installation process and operation prior to spudcan extraction. This note reports results from a series of experiments with particle image velocimetry (PIV) measurements (White *et al.*, 2003) that were performed in a drum centrifuge to facilitate observation of the effects of a load-hold period on the soil movements around a model spudcan, including during subsequent further loading.

Manuscript received 9 January 2014; revised manuscript accepted 14 October 2014. Published online ahead of print 21 November 2014. Discussion on this paper closes on 1 April 2015, for further details see p. ii.

* Centre for Offshore Foundation Systems and ARC CoE for Geotechnical Science and Engineering, University of Western Australia, Perth, WA, Australia.

## EXPERIMENTAL SET-UP AND PROCEDURE

### *Apparatus*

This investigation was conducted using the drum centrifuge at the University of Western Australia (UWA) (Stewart *et al.* (1998)). Half of a model spudcan with diameter, $D = 50$ mm and geometry similar to those utilised in the field (Fig. 2) was used to represent a jack-up footing. Under accelerations of 200***g*** the model represented a prototype diameter of 10 m.

The half footing was placed against the transparent acrylic window of a strongbox. A closed cell foam seal was bonded to the mating surface of the footing and was lubricated with petroleum jelly. This served to allow the footing to move smoothly along the surface of the window with minimal frictional resistance, while maintaining a seal between the footing and window of the strongbox.

The PIV measurements were captured using the system described by Stanier & White (2013). In brief, this system consists of a machine vision camera (AVT Prosilica GC2450C) with 5-megapixel resolution, large light-emitting diode (LED) panels for illumination, fibre-optic rotary joint for the transfer of data from the centrifuge to the control room in-flight and custom control software. Images were captured at a rate of 5 frames/s.

### *Sample preparation*

Commercially available kaolin clay was used to model the soil and two samples were normally consolidated under 200***g*** in the centrifuge. After consolidation and just prior to testing, the transparent acrylic window was carefully removed from the sample, allowing artificial seeding to be applied to the exposed surface of the model on which PIV measurements were conducted. The density of this seeding, or artificial seeding ratio (ASR), was optimised following the procedure proposed by Stanier & White (2013). This ensured

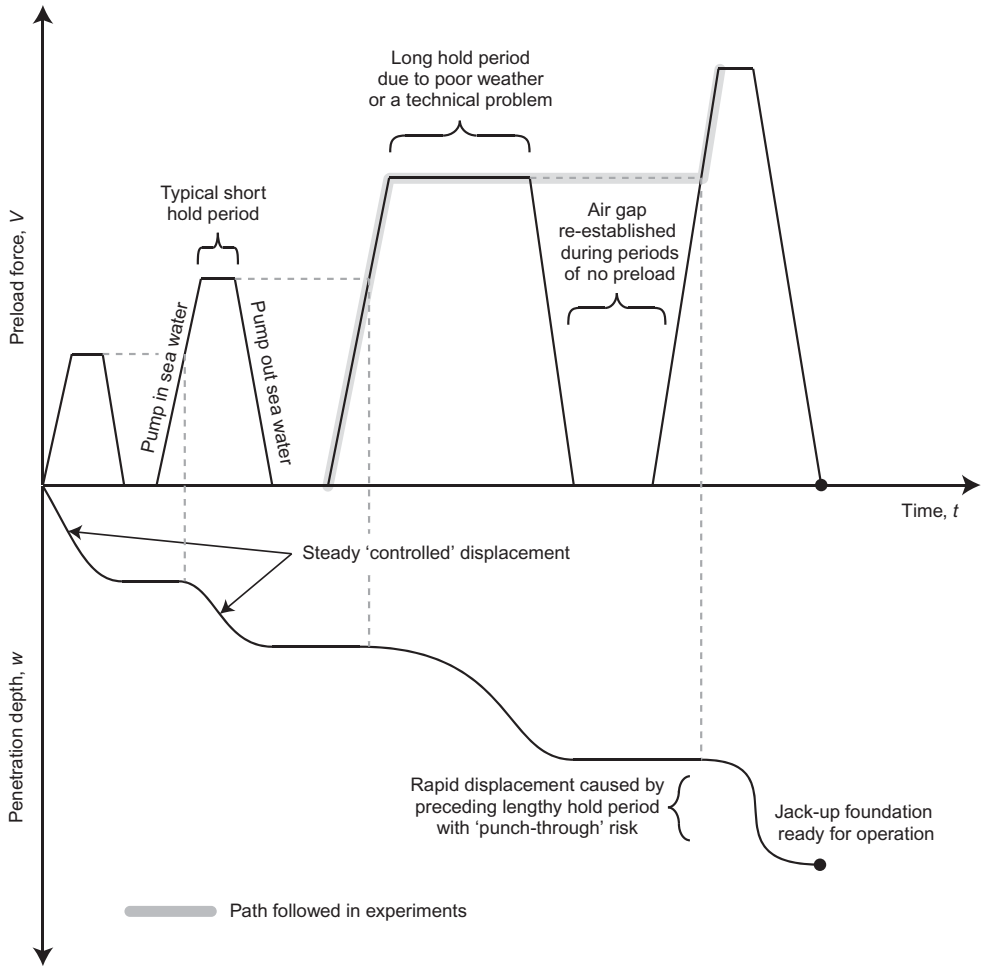


**Fig. 1. Typical time history of preload force and penetration during a discontinuous jack-up installation process**

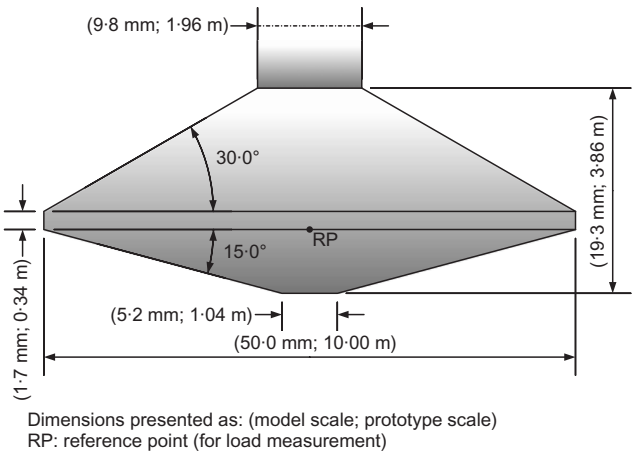


**Fig. 2. Schematic diagram of test process adopted and typical effect of a consolidation period on load–penetration curve observed in experiments**

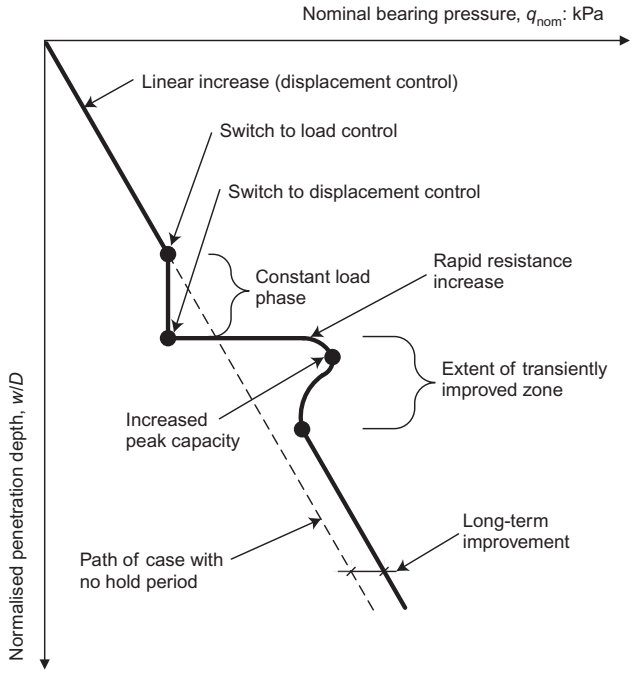


**Fig. 3. Dimensions of model spudcan footing**

that the PIV measurements were of an optimal precision for all tests.

*Test procedure and summary*

Figure 3 is a schematic diagram of the typical effect of a load-hold period on the bearing pressure-penetration response. The loading path being modelled here, with respect to the in-field condition, is also highlighted in Fig. 1. The initial stages of the tests were performed under displacement control at a constant rate until the reference point (taken as the lowest depth of the maximal diameter of the spudcan) reached either 0·5 or 1·0$D$. The penetration rate, $v$, was determined such that the normalised penetration rate, $vD/c_v$,

was 95, similar to the corresponding full model tests reported in Bienen & Cassidy (2013) and >30 to ensure undrained behaviour (Low *et al.*, 2008). The coefficient of consolidation, $c_v$, was taken as 2·6 m$^2$/year at 0·5$D$ depth and 3·5 m$^2$/year at 1·0$D$ after Bienen & Cassidy (2013).

After reaching the start depth for the load-hold period, the actuator was switched to load control (except for the reference case with no load-hold period). In this mode, feedback from a load cell on the shaft of the footing was used as an input to the actuator control software and the position of the actuator was constantly adjusted to maintain a near-constant reading on the load cell during the load-hold period. Following the load-hold period the actuator was switched back to displacement control at the same constant penetration rate as that used prior to the consolidation. The footing was then further penetrated until it had reached a total depth of 2·0$D$ (100 mm). Table 1 provides a summary of the tests performed, including key relevant test data.

Following spudcan testing, T-bar penetrometer (5 by 20 mm) tests were performed at 200***g*** in the two strongboxes used in the investigation (away from the footing test sites), which are presented in Fig. 4. By assuming an intermediate T-bar factor, $N_{T\text{-}bar}$ of 10·5 (Low *et al.*, 2008), a linear best fit was found with a mudline strength of 0·5 kPa and a prototype gradient of 1·6 kPa/m.

*Data analysis techniques*

For the tests with a load-hold period PIV analyses were performed using GeoPIV (White *et al.*, 2003) immediately following completion of the consolidation period and after further penetration equivalent to 0·25 and 0·5$D$. For comparison, companion analyses were performed at the same depths on images from the reference (no load-hold period) case. A patch size, $L$, equal to 50 pixels was found to give the best compromise between measurement precision and

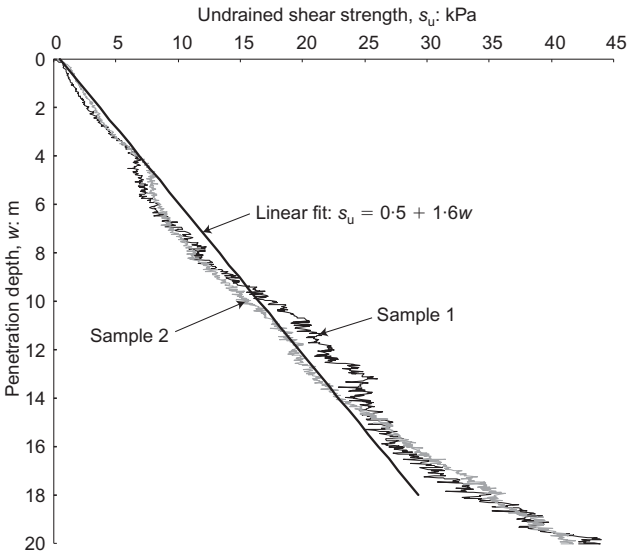


**Fig. 4. T-bar penetrometer profiles for the two strongboxes tested assuming $N_{T\text{-}bar} = 10{\cdot}5$**

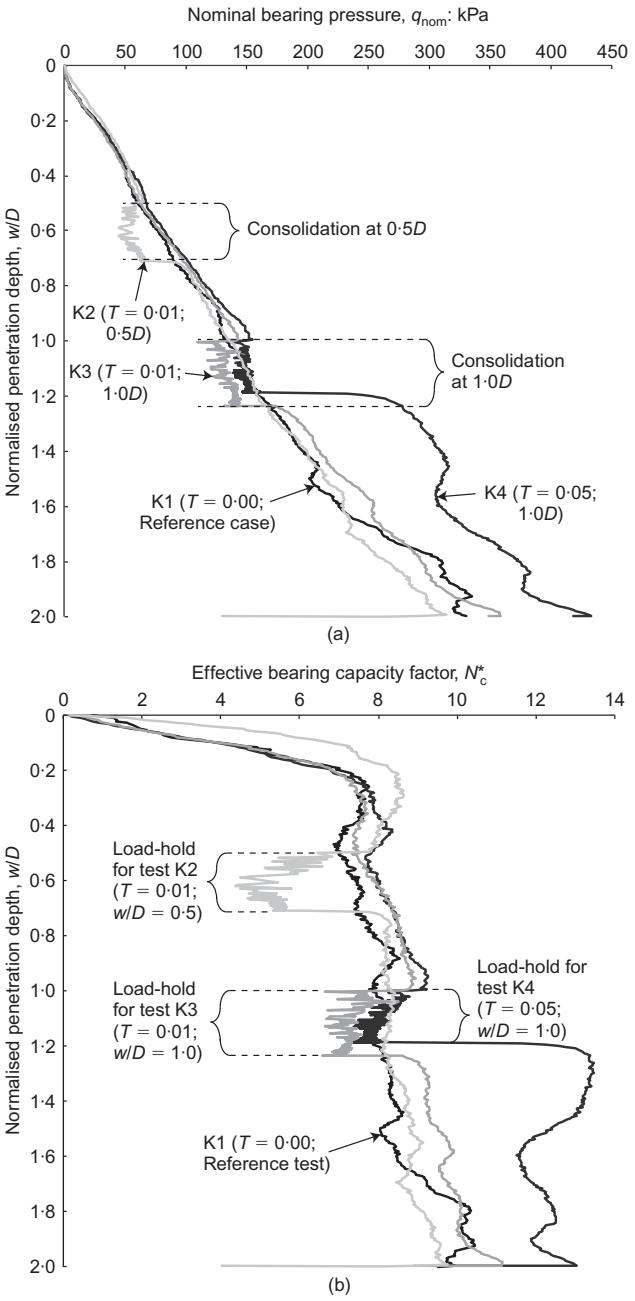


**Fig. 5. Profiles of (a) measured nominal penetration resistance ($q_{nom}$) and (b) back-calculated effective bearing capacity factor ($N_c^*$)**

**Table 1. Summary of tests performed**

| Load-hold period | | | | | Post load-hold period | | | |
|---|---|---|---|---|---|---|---|---|
| Test | Depth, $w/D$ | $T = c_v t/D^2$ | Average applied pressure: kPa | $\Delta w/D$ due to consolidation | Peak $N_c^*$ | $w/D$ at peak | Ref. $N_c^*$ | Peak $N_c^*$/ Ref. $N_c^*$ |
| K1 | N/A – Reference test | | | | | | | 1·00 |
| K2 | 0·5$D$ | 0·01 | 62·5 | 0·21 | 7·42 | 0·72 | 6·86 | 1·08 |
| K3 | 1·0$D$ | 0·01 | 138·3 | 0·23 | 8·11 | 1·25 | 7·45 | 1·09 |
| K4 | | 0·05 | 152·7 | 0·19 | 12·22 | 1·22 | 7·33 | 1·67 |

Note: $N_c$ is value of reference case at same penetration depth.

density. Patch spacing, $s$, of 10 was adopted in all analyses. Spurious vectors, which typically occurred within the penetration path due to sub-optimal texture caused by the remoulding of soil, were manually removed from the data set. Image space measurements (pixels) were converted to object space measurements (mm) using close-range photogrammetric correction after White *et al.* (2003).

## RESULTS AND DISCUSSION

The results shown in this paper are presented in non-dimensional or scale-independent forms. The following notation is used throughout: $q_{nom} = V/A$ is the nominal bearing pressure where $V$ is the vertical load and $A$ is the area of the spudcan in model scale. $w/D$ is the normalised penetration depth where $w$ is the penetration depth and $D$ is the spudcan diameter. $N_c^* = q_{nom}/s_u$ is the effective bearing capacity factor where $s_u$ is the original undrained shear strength from the T-bar fit at the relevant depth. $T = c_v t/D^2$ is the dimensionless consolidation time where $c_v$ is the coefficient of consolidation

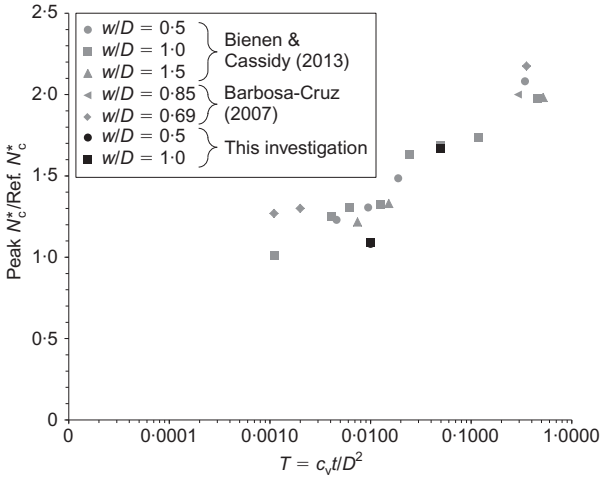


**Fig. 6. Effective bearing capacity factor ($N_c^*$) from PIV experiments compared to the data of Bienen & Cassidy (2013) and Barbosa-Cruz (2007)**

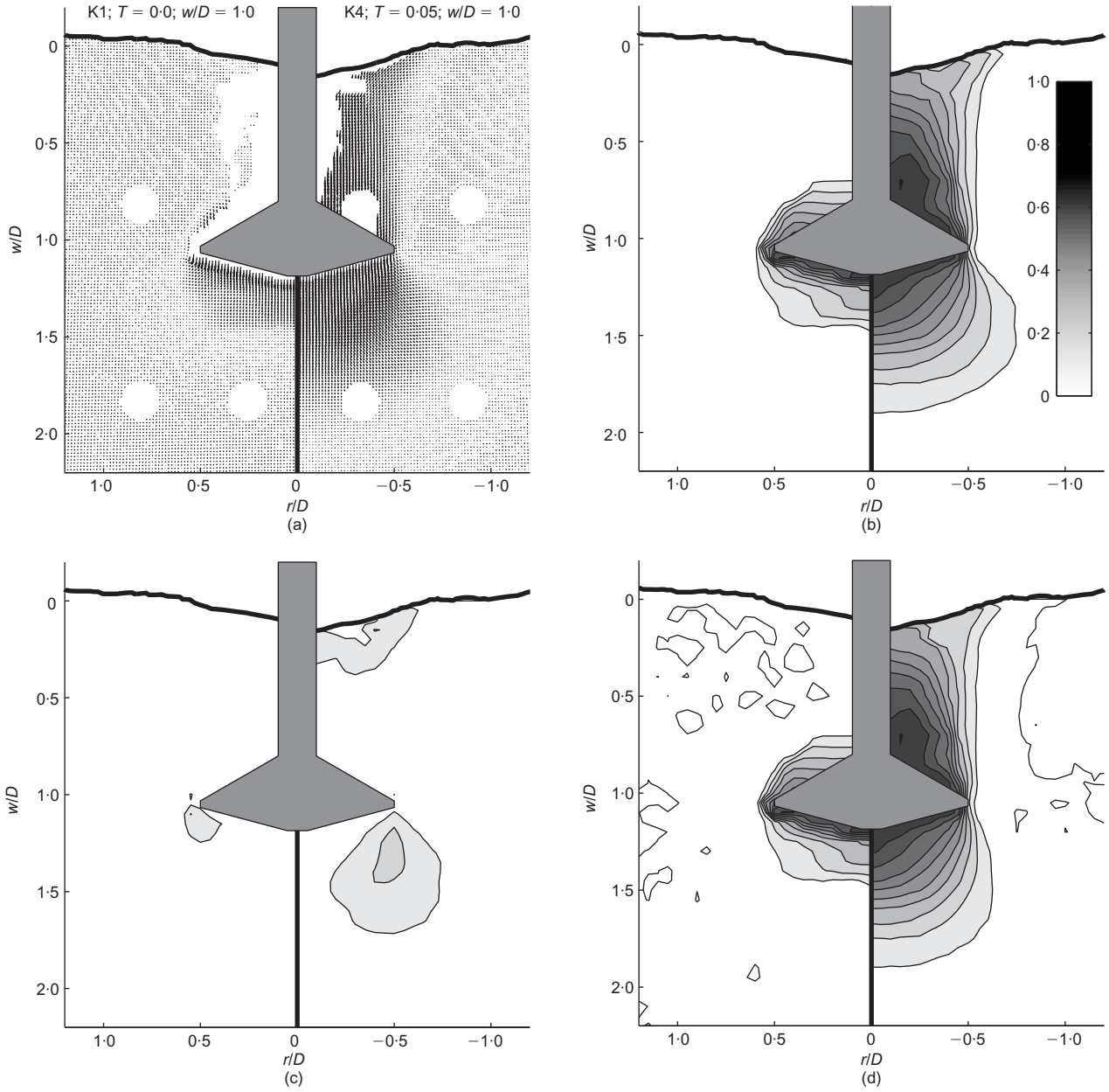


**Fig. 7. Comparison of velocity fields immediately following the load-hold period (LHS – no load-hold; RHS – with load-hold) for $T = 0{\cdot}05$ and $w/D = 1{\cdot}0$: (a) normalised vectorial velocities; (b) normalised resultant velocity contours; (c) normalised horizontal velocity contours; (d) normalised vertical velocity contours**

and $t$ is the dimensional time. PIV measurements are presented in the form of velocity fields, where $v_R$, $v_H$ and $v_V$ are, respectively, the resultant, horizontal and vertical velocities of the soil, which are normalised by the footing penetration velocity, $v_F$.

*Load-penetration response*

Figure 5(a) shows the measured penetration resistance, $q_{nom}$, with respect to penetration depth, while Fig. 5(b) presents the effective bearing capacity factor $N_c^*$. The penetration resistance increases linearly with depth until the onset of the load-hold period. Correspondingly the effective bearing capacity factor, $N_c^*$, increases initially very rapidly until a transition from shallow to deep failure occurs between 0·1 and 0·2$D$ – as predicted by Hossain & Randolph (2009). During the load-hold periods the footing continues to settle, hence $N_c^*$ reduces as the soil strength used to back-calculate $N_c^*$ rises. After the load-hold period, tests K2 and K3, where $T$ was 0·01 at $w/D$ of 0·5 and 1·0, respectively, show a similar enhancement in $N_c^*$ of 8–9% (peak $N_c^*$/ref. $N_c^*$ as noted in Table 1). In contrast, test K4 where $T$ was 0·05 at $w/D$ of 1·0, yielded an enhancement of $N_c^*$ of 67%. Fig. 6 shows that these enhancements are broadly comparable to those measured by Bienen & Cassidy (2013), providing some confidence in the efficacy of the PIV model-based measurements. In test K4, $N_c^*$ also remained ~20% higher for the remainder of the penetration than in the reference case of test K1, as occurred in similar tests reported by Bienen & Cassidy (2013).

*Velocity fields following a load-hold period*

The left-hand sides (LHS) and right-hand sides (RHS) of Figs 7, 8 and 9 compare the normalised velocity fields for tests K1 (no load-hold period) and K4 (the longest load-hold

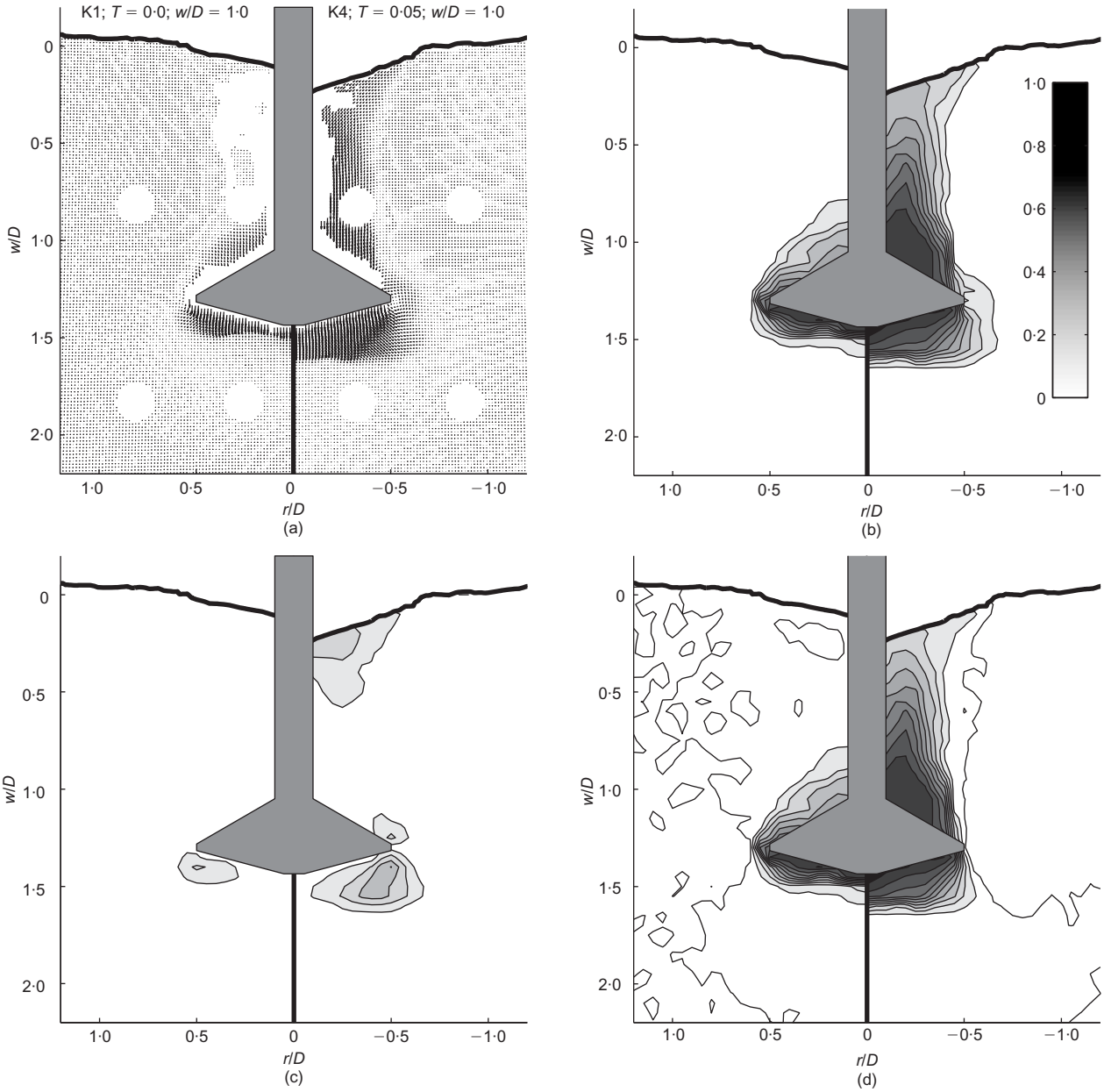


**Fig. 8. Comparison of velocity fields following 0·25$D$ penetration after following the load-hold period (LHS – no load-hold; RHS – with load-hold) for $T = 0·05$ and $w/D = 1·0$: (a) normalised vectorial velocities; (b) normalised resultant velocity contours; (c) normalised horizontal velocity contours; (d) normalised vertical velocity contours**

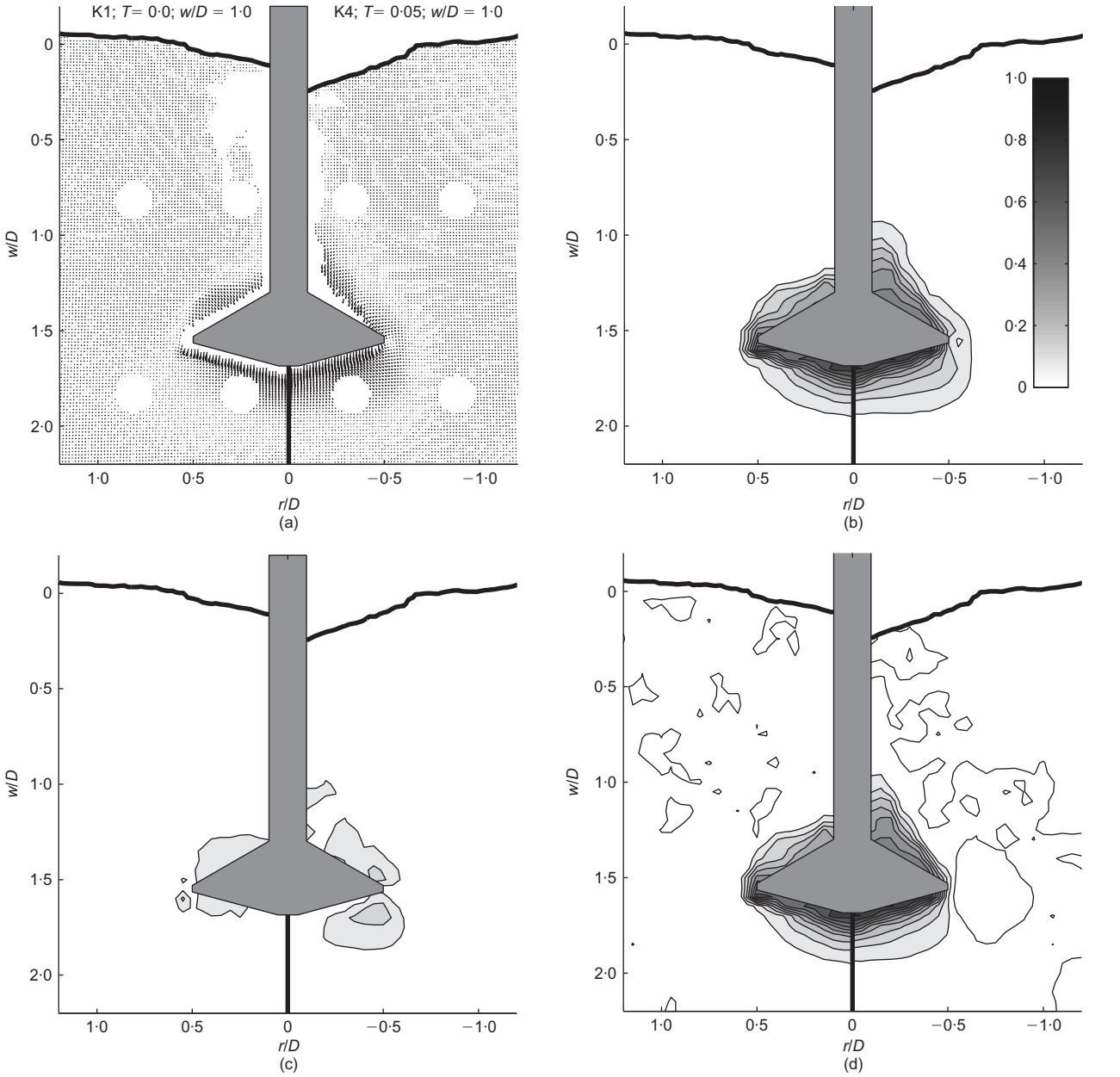


**Fig. 9. Comparison of velocity fields following 0·5*D* penetration after following the load-hold period (LHS – no load-hold; RHS – with load-hold) for $T = 0{\cdot}05$ and $w/D = 1{\cdot}0$: (a) normalised vectorial velocities; (b) normalised resultant velocity contours; (c) normalised horizontal velocity contours; (d) normalised vertical velocity contours**

where $T = 0{\cdot}05$ and initial embedment $w/D = 1{\cdot}0$) at depths following the end of the load-hold period of 0·0, 0·25 and 0·5*D*, respectively. Four sub-plots are used to illustrate the velocity fields at each depth: (*a*) normalised velocity vector field, (*b*) normalised contours of resultant velocity ($v_R/v_F$), (*c*) normalised contours of horizontal velocity ($v_H/v_F$) and (*d*) normalised contours of vertical velocity ($v_V/v_F$).

From these figures, the following observations can be made.

(*a*) Significantly more soil is mobilised by the spudcan immediately following a long load-hold period (K4) than for the reference case with no load-hold period (K1). This results in the greater penetration resistance evident in Fig. 5(a) and the initial peak in $N_c^*$ seen in Fig. 5(b).

(*b*) The extent of the soil mobilised in the load-hold period test (K4) reduces with increasing penetration, while for the reference case (K1) it is broadly consistent. The reduction in the extent of soil mobilised by further penetration mirrors the post-peak reduction in $N_c^*$ seen in Fig. 5(b).

(*c*) The similarity in the extent of the velocity fields at a depth of 0·5*D* following the end of this relatively long load-hold period (Fig. 9), coupled with the remaining 20% enhancement of $N_c^*$, implies that the load-hold period caused a general strengthening of soil in the vicinity of the spudcan. This must be caused by localised consolidation of soil, as indicated by the pore pressure dissipations measured at the spudcan tip by Bienen & Cassidy (2013). Efforts made to measure the volumetric strains (and infer changes in voids ratio) were unfortunately unreliable due to degradation of soil texture immediately beneath the footing, during the load-hold period.

These observations indicate that both the mechanism of soil movement and localised consolidation impact upon penetration resistance. The mechanism of soil movement has the strongest

influence on the initial (or peak) enhancement of penetration resistance for this long load-hold period. However, consolidation of a significant volume of soil beneath the footing, causing it to strengthen and stiffen, likely results in the offset in the penetration resistance from the reference case with no load-hold period. This latter effect is only apparent for relatively long, dimensionless, load-hold periods.

*Effects of dimensionless time and footing penetration depth*

Figures 10 and 11 present the velocity fields immediately following the end of the shorter load-hold period for tests K2 and K3 ($T = 0{\cdot}01$ at $w/D = 0{\cdot}5$ and $1{\cdot}0$, respectively). The significantly reduced extent of the velocity fields and magnitude of the enhancement in $N_c^*$ for both cases compared to test K4 (where $T = 0{\cdot}05$ at $w/D = 1{\cdot}0$), indicates that it is the dimensionless consolidation time, $T$, that dominates the initial enhancement of $N_c^*$ over the reference case, as opposed to the initial embedment depth, $w/D$. This is corroborated by the data of Bienen & Cassidy (2013) in Fig. 6, where no trend with initial embedment is evident.

## CONCLUDING REMARKS

A short series of centrifuge PIV experiments has been reported, investigating the impact of sustained loading on spudcan footings in clay. Short load-hold periods cause a modest increase in penetration resistance compared to a reference case with no load-hold period, due to the mobilisation of additional soil on the application of further loading. Longer load-hold periods exacerbate this effect; in addition, they cause an offset in penetration resistance of up to 20%, which remains evident even after further penetration of up to $0{\cdot}5D$. This implies that the soil surrounding the footing undergoes significant consolidation during the load-hold period. The observations presented in this note might help to validate methods to predict the enhancement in bearing

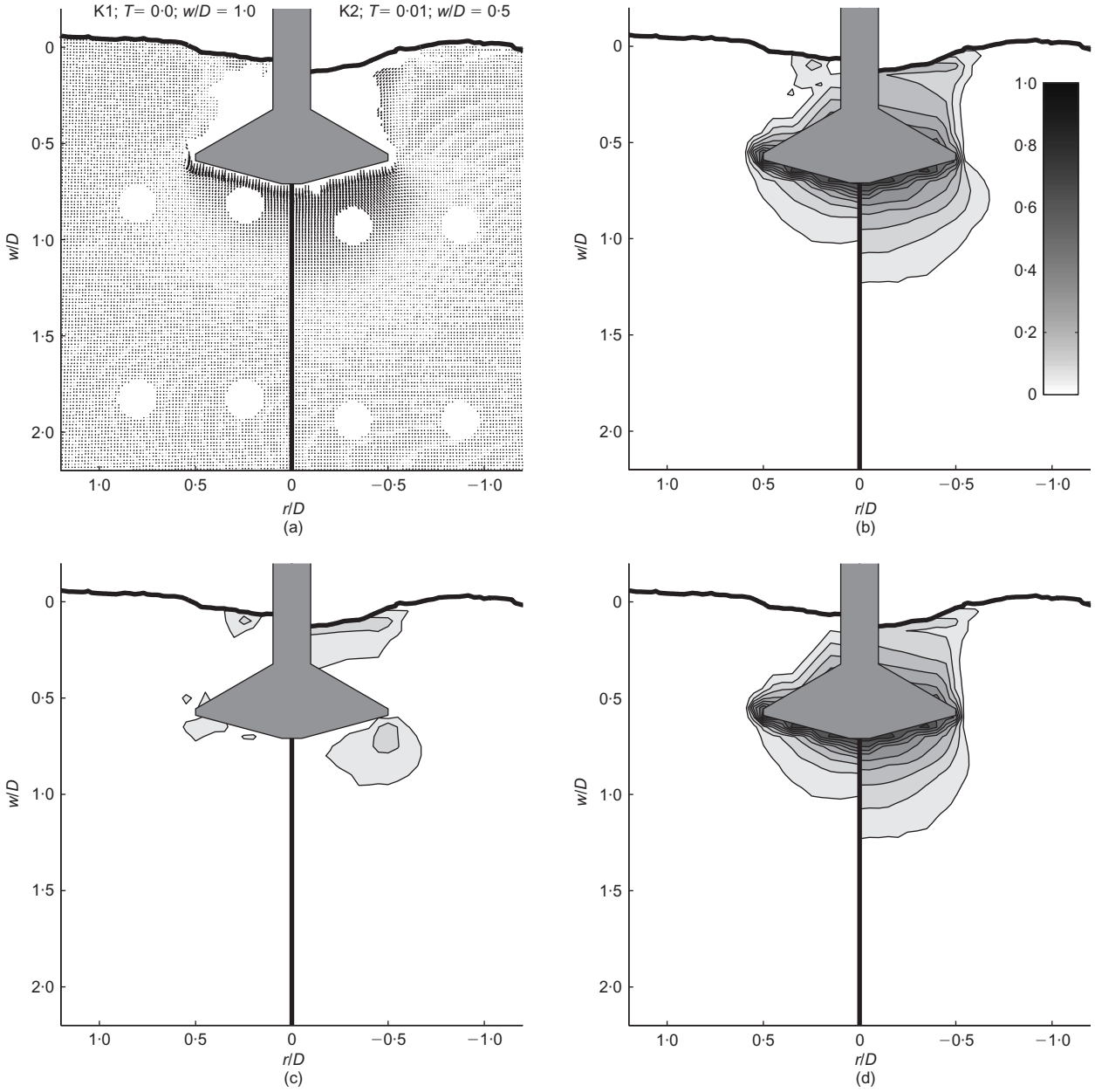


**Fig. 10. Comparison of velocity fields immediately following the load-hold period (LHS – no load-hold; RHS – with load-hold) for $T = 0{\cdot}01$ and $w/D = 0{\cdot}5$: (a) normalised vectorial velocities; (b) normalised resultant velocity contours; (c) normalised horizontal velocity contours; (d) normalised vertical velocity contours**

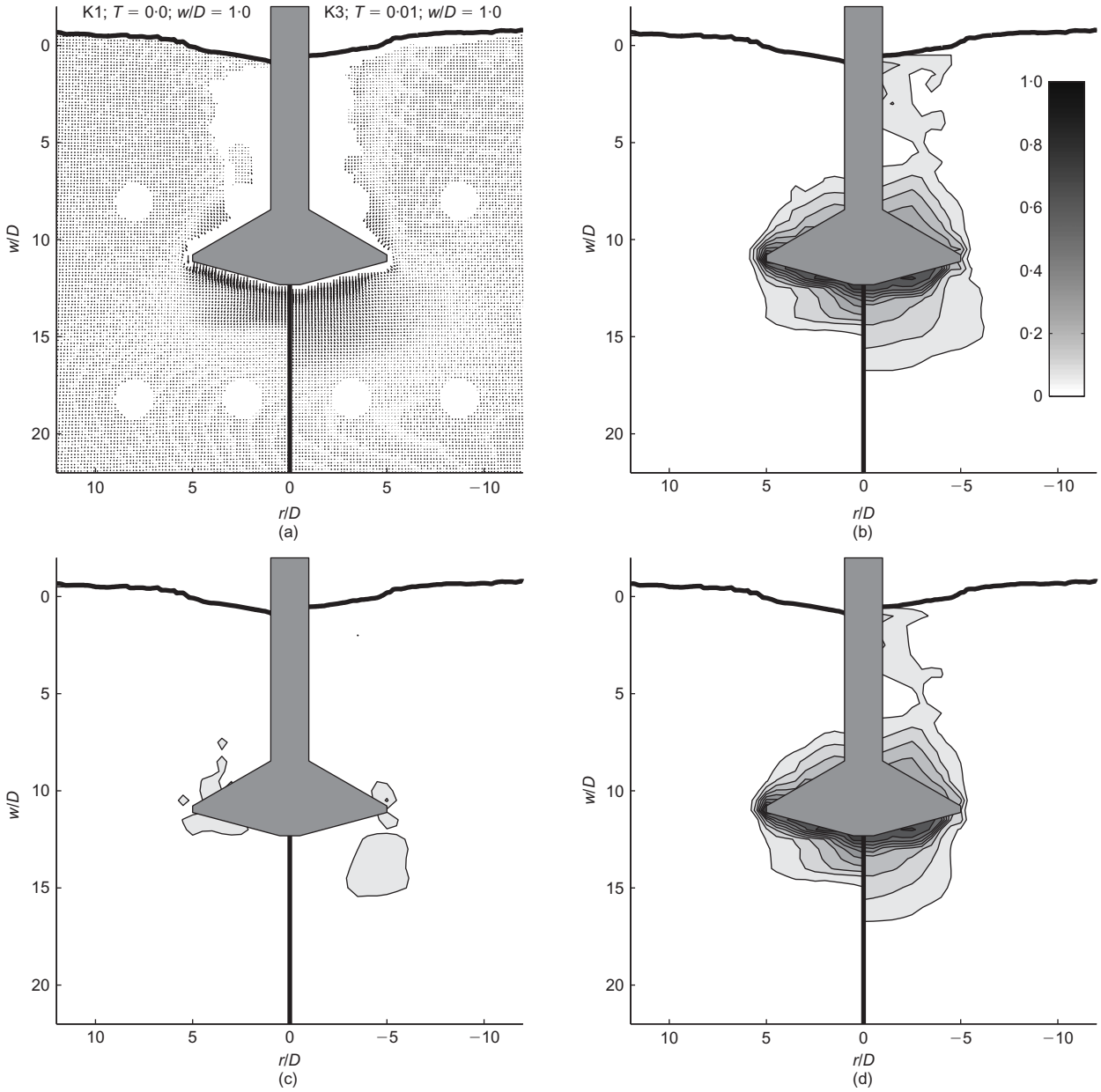


**Fig. 11. Comparison of velocity fields following 0·5*D* penetration after the load-hold period (LHS – no load-hold; RHS – with load-hold) for $T = 0{\cdot}01$ and $w/D = 1{\cdot}0$: (a) normalised vectorial velocities; (b) normalised resultant velocity contours; (c) normalised horizontal velocity contours; (d) normalised vertical velocity contours**

capacity factor due to a load-hold period during installation or operation (e.g. Bienen & Cassidy, 2013).

ACKNOWLEDGEMENTS

This work forms part of the activities of the Centre for Offshore Foundation Systems (COFS), currently supported as a node of the Australian Research Council Centre of Excellence for Geotechnical Science and Engineering and as a Centre of Excellence by the Lloyd's Register Foundation. Lloyd's Register Foundation, a UK registered charity and sole shareholder of Lloyd's Register Group Ltd, invests in science, engineering and technology for public benefit, worldwide. The third and fourth authors are the recipients of an Australian Research Council (ARC) Postdoctoral Fellowship (DP110101603) and Laureate Fellowship (FL130100059), respectively. This support is gratefully acknowledged.

NOTATION

| | |
|---|---|
| $A$ | spudcan area |
| $c_v$ | coefficient of consolidation |
| $D$ | spudcan diameter |
| $L$ | PIV analysis patch size |
| $N_c$ | bearing capacity factor |
| $N_c^*$ | effective bearing capacity factor |
| $N_{T\text{-bar}}$ | bearing capacity factor for T-bar |
| $q_{nom}$ | nominal bearing pressure |
| $s$ | patch spacing |
| $s_u$ | undrained shear strength |
| $T$ | dimensionless consolidation time |
| $t$ | dimensional time |
| $V$ | vertical force |
| $v$ | penetration rate |
| $v_F$ | footing penetration velocity |
| $v_H$ | horizontal soil velocity |
| $v_R$ | resultant soil velocity |
| $v_V$ | vertical soil velocity |
| $w$ | penetration depth |

REFERENCES

Barbosa-Cruz, E. R. (2007). *Partial consolidation and breakthrough of shallow foundations in soft soil*. PhD thesis, The University of Western Australia, Perth, WA, Australia.

Bienen, B. & Cassidy, M. J. (2013). Set-up and resulting punch-through risk of jack-up spudcans during installation. *J. Geotech. Geoenviron. Engng, ASCE* **139**, No. 12, 2048–2059, http://dx.doi.org/10.1061/(ASCE)GT.1943–5606.0000943.

Brennan, R., Diana, H., Stonor, R. W. P., Hoyle, M. J. R., Cheng, C. P., Martin, D. & Roper, R. (2006). Installing jackups in punch-through sensitive clays. *Proceedings of the offshore technology conference*, Houston, TX, paper OTC 18286.

Hossain, M. S. & Randolph, M. F. (2009). New mechanism-based design approach for spudcan foundations on single layer clay. *J. Geotech. Geoenviron. Engng***135**, No. 9, 1264–1274.

ISO (International Organisation for Standardisation) (2012). ISO/FDIS 19905-1: Petroleum and natural gas industries – Site-specific assessment of mobile offshore unit – Part 1: Jack-ups. Geneva, Switzerland: ISO.

Low, H. E., Randolph, M. F., DeJong, J. T. & Yafrate, N. J. (2008). Variable rate full-flow penetration tests in intact and remolded soil. In *Proceedings of the 3rd international conference on geotechnical and geophysical site characterization* (eds A.-B. Huang and P. W. Mayne), pp. 1087–1092. London, UK: Taylor and Francis.

Stanier, S. A. & White, D. J. (2013). Improved image-based deformation measurement in the centrifuge environment. *Geotech. Testing J.* **36**, No. 6, 915–927, http://dx.doi.org/10.1520/GTJ20130044.

Stewart, D. P., Boyle, R. S. & Randolph, M. F. (1998). Experience with a new drum centrifuge. In *Proceedings of the international conference centrifuge 98*, Tokyo, Japan (eds T. Kimura, O. Kusakabe and J. Takemura), vol. 1, pp. 35–40. Rotterdam, the Netherlands: Balkema.

White, D. J., Take, W. A. & Bolton, M. D. (2003). Soil deformation measurement using particle image velocimetry (PIV) and photogrammetry. *Géotechnique* **53**, No. 7, 619–631, http://dx.doi.org/10.1680/geot.2003.53.7.619.